NASA SP-8122

NASA
SPACE VEHICLE
DESIGN CRITERIA
(ENVIRONMENT)

THE ENVIRONMENT OF TITAN (1975)

JULY 1976

NATIONAL AERONAUTICS AND SPACE ADMINISTRATION

FOREWORD

NASA experience has indicated a need for uniform criteria for the design of space vehicles. Accordingly, criteria have been developed in the following areas of technology:

Environment
Structures
Guidance and Control
Chemical Propulsion

Individual components of this work are issued as separate monographs as soon as they are completed. A list of the titles that have been published can be found at the end of this monograph.

These monographs are to be regarded as guides to design and not as NASA requirements except as may be specified in formal project specifications. It is expected, however, that the monographs will be used to develop requirements for specific projects and be cited as the applicable documents in mission studies or in contracts for the design and development of space vehicle systems.

This monograph was prepared under the cognizance of the Goddard Space Flight Center with Scott A. Mills as program coordinator. The principal author was Calvin P. Myers of the Jet Propulsion Laboratory. Valuable contributions were made by A. J. Beck and Neil Divine of the Jet Propulsion Laboratory. Several others contributed greatly through discussions and by making material available prior to publication, particularly: John Caldwell, Princeton University; F. C. Gillett, Kitt Peak National Observatory; D. M. Hunten, Kitt Peak National Observatory; Tobias Owen, State University of New York at Stoney Brook; S. S. Prasad, Jet Propulsion Laboratory; and R. C. Whitten, Ames Research Center.

Comments concerning the technical content of these monographs will be welcomed by the National Aeronautics and Space Administration, Goddard Space Flight Center, Systems Reliability Directorate, Greenbelt, Maryland 20771.

July 1976

CONTENTS

1. INTRODUCTION 1

2. STATE OF THE ART 1
   2.1 Physical Data 1
      2.1.1 Orbit and Composition 2
      2.1.2 Mass and Radius 2
   2.2 Atmosphere and Models 2
      2.2.1 Theory 3
      2.2.2 Visual and UV Photometry and Polarimetry 3
      2.2.3 Near Infrared Spectroscopy 5
      2.2.4 Thermal Infrared Spectrophotometry 7
      2.2.5 Atmosphere Models in Recent Literature 8
         2.2.5.1 Caldwell Model 10
         2.2.5.2 Hunten Model 10
         2.2.5.3 "New" Model 12
      2.2.6 Engineering Models of Titan's Atmosphere 12
   2.3 Non-Gaseous Constituents 17
      2.3.1 Aerosols and Dust 17
      2.3.2 Clouds 17
   2.4 Surfaces 19
   2.5 Temperature Variations and Atmospheric Dynamics 20
   2.6 Upper Atmosphere and Ionosphere 20

3. CRITERIA 21
   3.1 Physical Data 21
   3.2 Model Atmospheres 21
   3.3 Non-Gaseous Constituents 22
   3.4 Surfaces 24
   3.5 Temperature Variations and Atmospheric Dynamics 27
   3.6 Upper Atmosphere and Ionosphere 27

REFERENCES 28

APPENDIX A. ATMOSPHERIC STRUCTURE RELATIONS 33

APPENDIX B. SYMBOLS 34

APPENDIX C. GLOSSARY 35

NASA SPACE VEHICLE DESIGN CRITERIA MONOGRAPHS 37

THE ENVIRONMENT OF TITAN (1975)

1. INTRODUCTION

Recent advances in knowledge of Titan have generated considerable interest in this satellite of Saturn and possible missions to investigate its environment. It is the smallest body in the solar system known to possess a substantial atmosphere. This atmosphere has the largest methane to hydrogen ratio of all reducing atmospheres observed thus presenting an environment similar to that which is presumed to have existed on primitive Earth at the origin of life. In terms of spacecraft entry dynamics, it has the most accessible atmosphere in the solar system and is possibly the only body with an atmosphere beyond Mars having a surface that lander spacecraft can reach.

Information about Titan has been derived primarily from ultraviolet and infrared spectroscopic and infrared and microwave radiometric observations. The data are limited by the angular and spectral resolutions possible with Earth-based instrumentation and sensors on aircraft, rockets, balloons and Earth-orbiting satellites.

This monograph provides physical characteristics and atmospheric models necessary to support design and mission planning of spacecraft that are to orbit Titan, enter its atmosphere or land on its surface. The atmosphere affects the orbital lifetime, the flight dynamics, and performance of the spacecraft. Effective investigation of Titan by a probe or lander requires a detailed quantitative description of the atmosphere to predict and control thermal and electrical interactions between the atmosphere and spacecraft. Design of the communications subsystem and evaluation of planetary quarantine measures also require knowledge of the atmospheric environment.

This monograph includes data available through June 1975. It updates and expands a report, Titan Atmosphere Models (1973) (JPL TM 33-672), that incorporated pertinent information from the Titan Atmosphere Workshop held at the Ames Research Center, Moffett Field, CA, on 25-27 July 1973.

2. STATE OF THE ART

2.1 Physical Data

The data necessary for understanding the physical nature of Titan are discussed in the following paragraphs. Essential data pertaining to Saturn are available in The Planet Saturn (1970) (NASA SP-8091). Photometric and spectroscopic properties which pertain to Titan's atmosphere and surface are discussed in detail in sections 2.2.1 through 2.2.4.

2.1.1 Orbit and Composition

Titan, the sixth and largest satellite of Saturn, has a radius slightly larger than that of Mercury. Its rotation is assumed synchronous with its revolution about Saturn, and its pole perpendicular to its orbit (in Saturn's equatorial plane). Thus, Titan's "day" is 16 Earth days. Titan's "year", 30 Earth years long, has 675 "days". Its "seasons" result from an inclination of 27° (comparable to Earth's) and its variation in heliocentric distance (9.0 to 10.1 AU). Current theories suggest that its structure, similar to that of some other large satellites of the outer planets, includes a rocky, muddy core, a liquid (H_2O solution) mantle (most of the volume), possibly an ice crust, and an atmosphere (ref. 1). The last characteristic may be unique to Titan on both theoretical and observational grounds.

2.1.2 Mass and Radius

Accurate mass and radius determinations are essential for an understanding of the physical nature of Titan. Evaluation of the mean density and surface gravity depends on both parameters, and interpretation of photometric observations in terms of albedo and brightness temperatures requires the radius. The mass of Titan has been determined by several investigators to within about 1% by observing perturbations in the orbit of Hyperion (the 7th satellite of Saturn) which is resonant with the orbit of Titan (ref. 2). The mass determined in this manner is $M = (1.37 \pm 0.02) \times 10^{23}$ kg.

Accurate radius measurements, in contrast to mass measurements, are very difficult because the apparent diameter of Titan as seen from Earth is only about 0.7 arcsec. Measurements of the apparent visual diameter give a physical diameter of about 4850 ± 300 km (ref. 2). Because of the large uncertainty and difficulties in assessing systematic errors, a radius of 2500 km ± 250 km was adopted by the Titan Workshop in 1973 (ref. 3). Recent lunar occultation observations (ref. 4) have provided more precise values of the diameter. Details of these observations are not yet available, but the result is 5800 ± 200 km. This value corresponds to a level in the atmosphere near an optical depth of unity, perhaps about 200 to 300 km above the surface. In this monograph values of R_a = 2900 ± 100 km for the effective radius of Titan's atmosphere and R_s = 2700 ± 200 km for the surface radius have been adopted to be consistent with the lunar occultation observations. The greater uncertainty in surface radius reflects the uncertainty in attempting to specify a location for the surface. The mass, radius, and other physical parameters are given in table 3 (sec. 3.1).

2.2 Atmosphere and Models

The considerations that establish the presence and properties of Titan's atmosphere are summarized in sections 2.2.1 through 2.2.4.

2.2.1 Theory

The relatively large mass, modest radius, and low effective temperature of Titan permit retention of several candidate atmospheric gases for times comparable to the age of the solar system. Light gases ($u \leqslant 4$ g/mole, namely hydrogen and helium) cannot be retained in substantial quantities (refs. 5, 6, and 7) unless they are mixed with heavier gases, replenished as they escape, or are recycled through Titan's atmosphere from a torus that is composed of escaping molecules captured in orbit around Saturn (refs. 8 and 9). Heavier gases are more likely candidates for the atmosphere. Their loss rates, which depend on photodissociation in the upper atmosphere, may be sufficiently small that these gases are relatively stable. On the basis of solar abundance, the candidate gases include CH_4, NH_3, H_2O, H_2S, N_2, and the inert gases other than He. Adequate sources of these and some other volatiles exist in the bulk material of Titan (ref. 1) and could replenish the atmosphere if suitable release or synthesis processes are active. However, H_2O and NH_3 condense at sufficiently high temperatures that they would not be found in substantial quantities in the atmosphere.

Other gaseous and non-gaseous atmospheric constituents such as aerosol or dust are probably present from photolysis and polymerization of the major atmospheric components (refs. 10 and 11) and meteoritic infall. If such products are present to any appreciable extent, they would modify many of the physical characteristics of the surface and atmosphere.

In the upper strata of the atmosphere above the regions of significant radiation reflection and emission, photodissociation and photoionization probably result in an ionosphere. The electron and ion densities and temperatures of this region depend on neutral molecular concentrations as well as ion production and recombination rates (ref. 12). Lower in the atmosphere, significant electron and ion densities may occur from ionization by cosmic rays (ref. 13) (sec. 2.6).

2.2.2 Visual and Ultraviolet Photometry and Polarimetry

Titan's spectral reflectance shown in figure 1 is characterized by two main features, one in the ultraviolet region of the spectrum and the other at visual wavelengths (ref. 20). The ultraviolet region is characterized by a very low reflectivity according to reference 14 and Caldwell.* At visual wavelengths the spectrum is distinctly similar to that of Saturn's equatorial band (ref. 16) although Titan's albedo is much lower than Saturn's. This similarity has been attributed to a chromophore, possibly a photolysis product of CH_4 that is common to Titan's atmosphere or surface and Saturn's atmosphere. Quantitative differences between the spectra and between the albedos of Titan and Saturn's equatorial belt can probably be accounted for by differences in methane-hydrogen ratios and chromophore concentration. To obtain geometric albedo as a function of wavelength, the

*Caldwell, John, "Ultraviolet Observations of Small Bodies in the Solar System by OAO-2," Icarus, Vol. 25, No. 3, 1975, pp. 384-396.

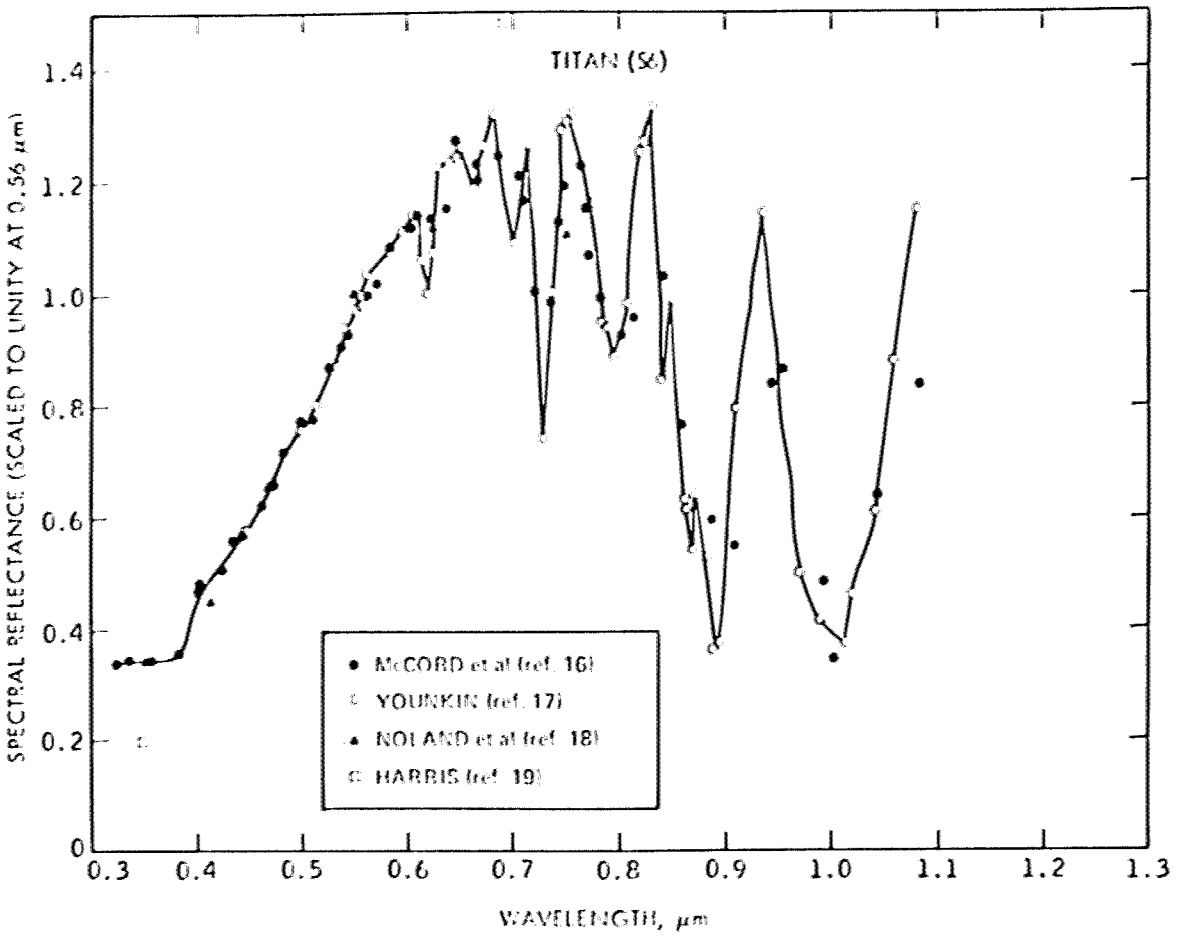

Figure 1. Spectral Reflectance of Titan. Lines have been drawn between Younkin's data points. (reference 20)

values in figure 1 (refs. 16, 17, 18 and 19) should be multiplied by 0.15, the geometric albedo at 0.56 μm (ref. 20).

Photometry and polarimetry at visual and ultraviolet wavelengths give some information about the atmospheric composition, thermal structure, presence of clouds, and possibly Titan's surface.

Owen and Cess (ref. 21) have estimated the atmospheric CH_4 abundance from absorption lines in the visible spectrum at 0.486, 0.543, and 0.576 μm by using a band model and extrapolating from Jupiter's relatively well known CH_4 abundance (ref. 22). Their estimate employed Trafton's pressure-abundance product (sec. 2.2.3) Lutz et al. (ref. 23) subsequently revised this estimate by using laboratory band strengths to determine the abundance density. They estimated approximately 0.08 km Agt with a corresponding surface pressure of 400 mb. The high pressure and small CH_4 abundance require the presence of another gas in the atmosphere. Owen and Cess propose either neon or

nitrogen to produce the pressure required by their observations: 34 km Agt of Ne, 25 km Agt of N_2, or 15 km Agt of each in an equal mixture (refs. 21 and 24). Ammonia (NH_3) has not been detected in Titan's visible spectrum. A current upper limit for the NH_3 abundance is 4×10^{-4} km Agt (ref. 22).

At short wavelengths ($\lambda \leqslant 0.4\ \mu m$), the low spectral reflectance indicates the existence of an absorber high in the atmosphere (refs. 14, 26, 27, 28, 15, and 29). A temperature inversion is attributed to this absorber (sec. 2.2.4). The absorber is assumed to be particles sufficiently small that the emissivity is inversely related to wavelength. The layer absorbs solar radiation in the ultraviolet region and transfers thermal energy to CH_4 and other molecules that reradiate in the infrared.

There is inconclusive evidence of clouds in the atmosphere of Titan. Linear phase coefficients measured between 0° and 6° at wavelengths from 0.35 to 0.75 μ show no indication of a non-linear brightness surge close to opposition but do show an unusual wavelength dependence (ref. 30). There is no apparent brightness or color variation with orbital phase (ref. 31). These observations suggest the existence of an opaque cloud layer in Titan's atmosphere. Veverka (refs. 31 and 32) also interpreted his polarization measurements (the polarization is positive at all phase angles) as suggestive of clouds. A smooth glassy surface covered with hydrocarbon photolysis products might account for these measurements, however. Three-color polarimetric measurements were judged by Zellner (ref. 33) to be inconsistent with scattering from either an ordinary planetary surface or a pure molecular atmosphere but compatible with an opaque cloud layer. Also, long period variations in Titan's color and brightness have recently been detected (ref. 34, 35, and 36). Although they are not understood, such variations could arise from changes in clouds covering Titan's surface. However, if there is a large temperature inversion in Titan's atmosphere, cloud formation would be unlikely. In that case, surface properties and the high-altitude ultraviolet absorber would have to account for the foregoing photometric and polarimetric results.

2.2.3 Near Infrared Spectroscopy

Deep methane absorption bands dominate Titan's spectrum in the near infrared. Spectroscopy in this region provides information about the composition of the atmosphere in terms of molecular species and their abundances.

The absorption lines in Titan's spectrum that are identified conclusively as methane have been reported, analyzed, and re-evaluated (refs. 37, 38, 39, and 40). Trafton's detailed analysis of the R(5) manifold of the $3\nu_3$ band with the assumption of a pure CH_4 atmosphere gave a column abundance in excess of 1.6 km Agt; this agreed with previous estimates based on analysis of the Q branch. The abundance of 1.6 km Agt may be the total CH_4 in the atmosphere, or it may be the CH_4 in the portion of the atmosphere that lies above an opaque cloud layer.

Hydrogen has also been identified in Titan's spectrum. Trafton has identified an emission feature at 0.81507 μm as the S_3 (1) quadrupole line of H_2 (refs. 39 and 41). He has also tentatively identified a feature at 0.82727 μm as the S_3 (0) line of H_2. The H_2 abundance estimate from the equivalent line width at 0.81507 μm is 5 ±3 km Agt.

However, this value is highly suspect for two reasons. First, there is a large uncertainty in the measurement because the observed line width was near the instrument's detection limit. Second, large amounts of H_2 are unlikely to be retained by Titan because of its low gravity even if some H_2 is recaptured from a hydrogen torus (refs. 8 and 9).

Other minor atmospheric components have been identified in the infrared reflectance spectrum. Ethane (C_2H_6) has been identified by its ν_9 fundamental emission band at 12.2 μm (ref. 42). Acetylene (C_2H_2), ethylene (C_2H_4), and mono-deuterated methane (CH_3D) also have been tentatively identified on the basis of wavelength, emission line shape and probability of the molecule's presence in the atmosphere (ref. 42). Positive identification on the basis of wavelength and shape alone was not possible because of insufficient resolution in the data.

Table 1
Infrared Photometry of Titan

	Narrowband	
Range (μm)	Resolution $\Delta\lambda/\lambda$	Reference
8. – 13	0.015	Gillett *et al.* (ref. 43)
7.8 - 13.3	0.02	Gillett (ref. 42)
3.5 - 21	0.05 - 0.29	Knacke *et al.* (ref 44)
1.65 - 35	0.02 - 0.47	Low and Rieke (ref. 45)
	Broadband	
Effective Wavelength (μm)	Bandwidth (μm)	Reference
4.9	0.8	Joyce *et al.* (ref. 46)
8.4	0.8	Gillett *et al.* (ref. 43)
10.6	–	Low & Rieke (ref. 45)
11	2	Gillett *et al.* (ref. 43)
12	2	Gillett *et al.* (ref. 43)
12.4	4	Allen & Murdock (ref. 47)
21	–	Low & Rieke (ref. 45)

2.2.4 Thermal Infrared Spectrophotometry

Broad-band and narrow-band measurements of Titan's infrared flux or brightness temperature give information from which the atmospheric temperature and composition can be inferred. The wavelength range and resolution for narrowband measurements and the effective wavelength and bandwidth for broadband measurements of several recent investigations are given in table 1. Also brightness temperatures corresponding to many of these measurements are shown in figure 3.

In the absence of an internal heat source, the effective temperature of a body T_e is expected to equal the equilibrium temperature, i.e., the surface temperature which that body would reach when only the incoming solar flux and the total reflected flux (bolometric Band albedo) are considered. The albedo of Titan, $A_{bol} = 0.20$ (ref. 17), corresponds to an effective temperature of $T_e = 85 \pm 2$ K. Brightness temperatures in excess of 85 K indicate modification of Titan's heat budget by its atmosphere.

Titan's atmospheric thermal structure can be inferred from the relationship between brightness temperature and wavelength. Emission features from CH_4 and C_2H_6 indicate a warm stratosphere and suggest the presence of a thermal inversion. A brightness temperature of approximately 160 K from the 7.7 μm fundamental of CH_4 indicates the temperature of the inversion base (refs. 45, 15, and 9).

Abundance values for methane, ethane, and acetylene (C_2H_2) have been estimated from the infrared flux measurements between 8 and 13 μm (sec. 2.2.3). Caldwell (ref. 15) estimated an ethane abundance of 5×10^{-6} km Agt by using a random band model with ethane mixed throughout an isothermal atmosphere at 160 K and adjusting the abundance to fit the data point of Gillett et al. (ref 43) at 12.0 μm.* Caldwell also estimated 10^{-5} km Agt of acetylene by using the same method to fit the 13.0 μm measurement in reference 43. Figure 3 shows a comparison between the observed infrared emission and the emission calculated by Caldwell with these abundance estimates (sec. 2.2.5.1).

Absorption at 17 μm has not been observed in Titan's infrared spectrum (ref. 45). The absence of this absorption feature indicates a limited quantity of H_2 because a few km Agt of H_2 would cause pressure-induced absorption. This rules out a H_2-induced greenhouse effect and its attendant high surface temperatures. However, a weak greenhouse effect with slightly-elevated surface temperatures from pressure-induced absorption by CH_4 (ref. 49) or from quasipolar absorption by CH_4 (ref. 50) is consistent with the 8 to 20 μm measurements of Low and Rieke (ref. 45).

In contrast to the infrared measurements, microwave radiometric measurements at 3.7 cm (8085 MHz) should give the temperature at the surface of Titan as none of the proposed atmospheric constituents (ref. 51) are effective absorbers at that wavelength.

*Caldwell (ref. 15) scaled the data of Gillett et al. (ref. 43) to be consistent with a radius of 2900 km.

Measurements by Briggs (ref. 52) yielded a brightness temperature of 115 ± 40 K (100 ± 30 K for a surface radius of 2700 km) which tentatively favors high values for the surface temperature from a moderate (CH_4) greenhouse effect but does not exclude values as low as ~80 K. These results are consistent with the implications from infrared measurements.

2.2.5 Atmospheric Models in Recent Literature

Several numerical models of various aspects of Titan's atmosphere have appeared in the literature over the past few years. Those prior to July 1973 are summarized in NASA SP-340 (The Atmosphere of Titan, ref. 3) which contains the proceedings of a workshop held at Ames Research Center 25 to 27 July 1973. Additional models are presented by Divine (ref. 53) and Kessler and Myers (ref. 54).

Figure 2 illustrates the scientific models in more recent literature which are reviewed in sections 2.2.5.1 through 2.2.5.3. The models are used to specify the ranges of parameters used for generating the engineering models of Titan's atmosphere constructed in section 2.2.6. Table 2 lists the parameters for candidate atmospheres, taken from figure 2. The most prominent feature of the recent scientific models is a large temperature inversion

Table 2
Candidate Parameter Sets From Current Literature

Model	Major Constituents, Abundances and Molecular Weights	Pressure, *P* (mb)	Temperature, *T* (K)
Caldwell	Mostly CH_4	17	160 Isothermal
	1.6 km Agt	17	78 Surface
	u = 16 g/mole		
Hunten	Mostly CH_4 (N_2)	10^{-7}	110 Thermopause*
	2 km Agt above clouds	10^{-5}	100 Mesopause*
	22-36 km Agt below clouds	0.1	160 Inversion base
	u = 16 g/mole	10	76 Tropopause*
	(u = 28 g/mole if N_2 is major constituent)	220-360	125 Surface
"New"	Mostly N_2	1.9	160 Inversion base
	25 km Agt N_2	400	78 Surface
	0.08 km Agt CH_4		
	u = 28 g/mole		

*Defined in the Glossary, appendix C.

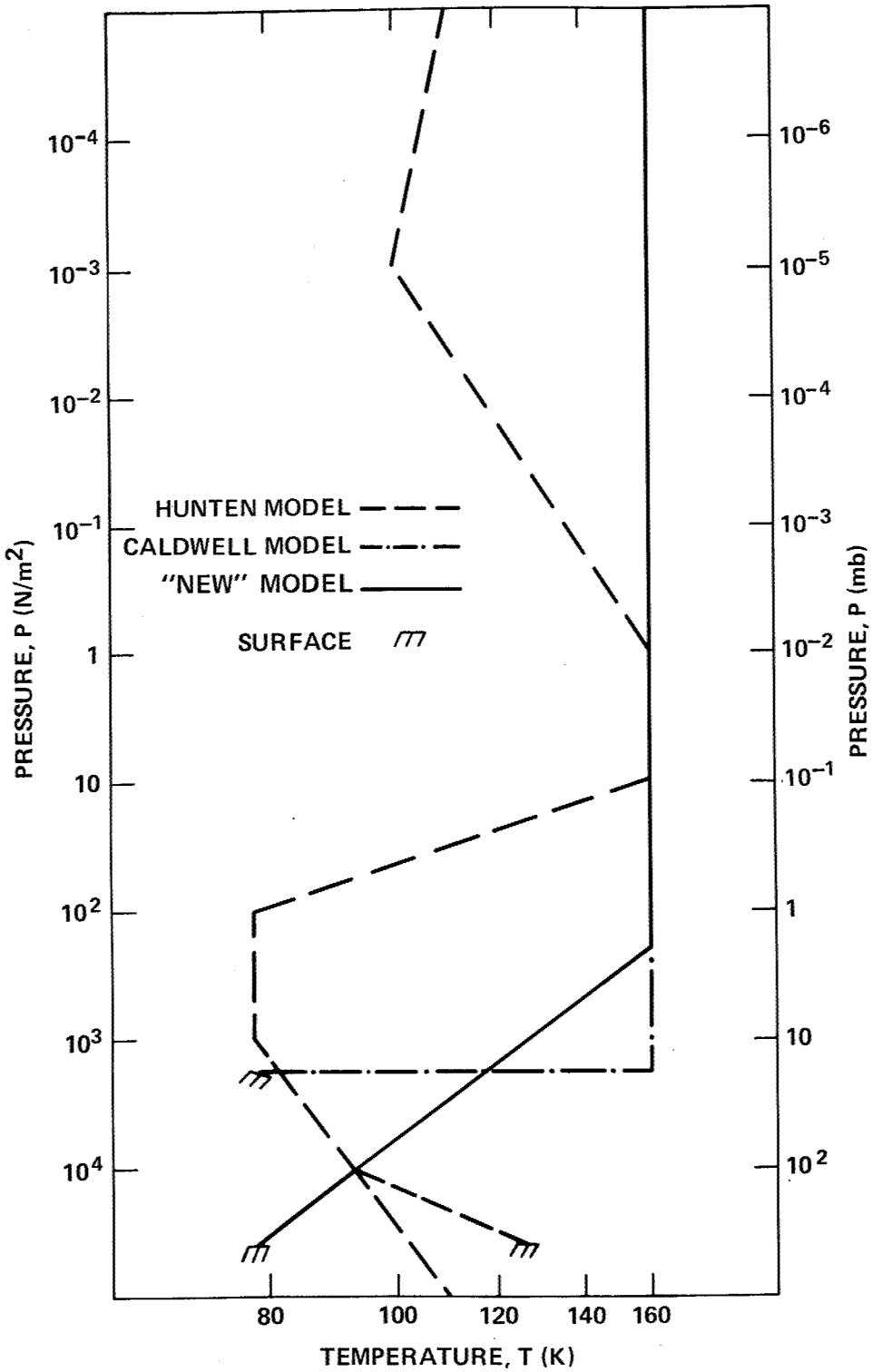

Figure 2. Pressure-Temperature Profiles of Models of Titan's Atmosphere Currently in the Literature and New Model to Reflect Recent Findings

which results in emission from CH_4 at 7.7 μm with a brightness temperature of 160 K. The temperature inversion is caused by small dust particles in the stratosphere which absorb solar ultraviolet radiation and thus cause a low ultraviolet albedo.

In an inversion model absorption of solar radiation (atmospheric heating) occurs high in the atmosphere. Below the absorption region temperature decreases with decreasing altitude ($dT/dZ > 0$). By contrast, a greenhouse model has an elevated surface temperature. Above the surface temperature decreases with increasing altitude ($dT/dZ < 0$) because the atmosphere is translucent to solar radiation but is opaque to infrared radiation from the surface. Although inversion and greenhouse models are very different, they are not mutually exclusive. In fact, the observed brightness temperatures (sec. 2.2.4) are consistent with both an inversion in the stratosphere and slightly elevated temperatures at the surface (refs. 45 and 9).

2.2.5.1 Caldwell Model

The model by Caldwell (ref. 15), represented in figure 2 by the alternating dash-dot line, is a revision of the original temperature inversion model by Danielson et al. (ref. 26). It has the minimum atmospheric abundance that is consistent with current observations. In the model all photometric and polarimetric properties of Titan are determined by the physical characteristics of stratospheric dust and surface because clouds are unlikely in a large temperature inversion. Brightness temperature calculations employ a surface radius of 2700 km and an atmospheric radius of 2900 km which are consistent with recent measurements (sec. 2.1.2). Because of uncertainties in the H_2 abundance determinations, Caldwell considered CH_4 to be the bulk constituent of the atmosphere. Therefore, the surface temperature determines the vapor pressure and hence the column abundance of CH_4. He calculated a surface temperature of 78 K which yields a pressure of 17 mb, is consistent with abundance measurements (sec. 2.2.3), and is consistent with energy balance considerations. The temperature throughout the atmosphere is 160 K from the 7.7 μm observations. Caldwell did not estimate a pressure for this region.

To illustrate that the inversion model accounts for all observed features in the infrared spectroscopic data, Caldwell compared predicted with observed infrared emission values. He used a black body model to calculate the infrared emissions from the surface at 78 K and from an optically-thin dust layer at 160 K. He used a random band model to calculate the emission at 160 K for abundances of 1.8 km Agt of CH_4, 5×10^{-6} km Agt of C_2H_6, and 10^{-5} km Agt of C_2H_2. Figure 3 compares the calculated and observed infrared emissions; the axes are drawn so that the area under the curve is proportional to the radiated power.

2.2.5.2 Hunten Model

In Hunten's model (ref. 9) which is represented by the dashed line in figure 2, the temperature inversion overlies a troposphere where the surface temperature is elevated by a weak greenhouse effect from pressure-induced CH_4 transitions. In contrast to Caldwell's

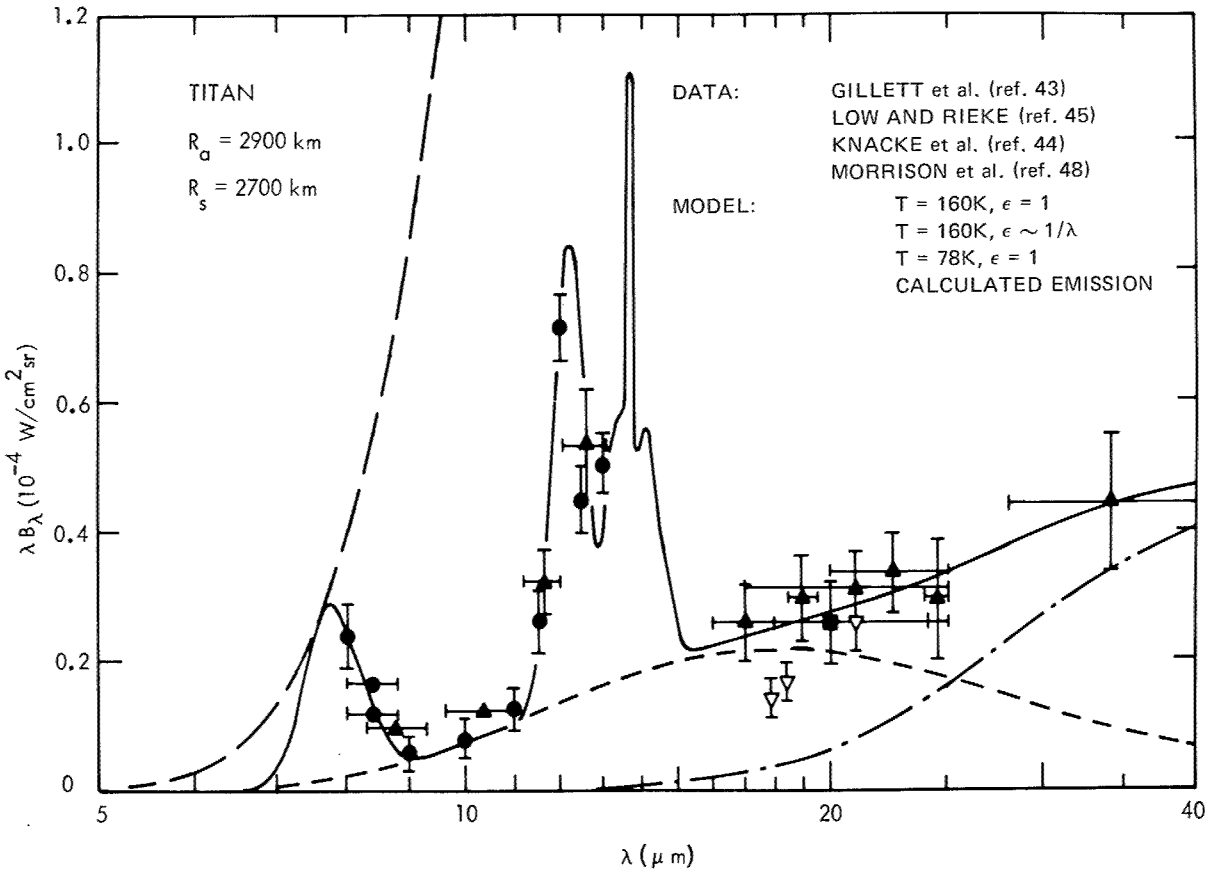

Figure 3. Comparison of Infrared Photometric Observations with Calculated Emission from the Temperature Inversion Model (reference 15)

model, clouds near the tropopause produce the photometric and polarimetric characteristics of Titan. The brightness temperatures are based on a radius of 2550 km and would be slightly lower if the radius of 2900 km adopted in this monograph were used.

Hunten selected the brightness temperature of 125 K at 10 μm as the most likely surface temperature. The atmosphere provides an attenuation (possibly pressure-induced CH_4 transitions) that results in the observed flux at 17 μm which corresponds to a 100 K brightness temperature. If the atmosphere is pure methane, at least 22 to 36 km Agt of additional CH_4 is required below the clouds to account for the opacity; this amount would produce surface pressures of 220 to 360 mb. If N_2 is assumed to be the primary bulk component, then the pressures would be about twice as high (395 to 630 mb). Above the surface the temperature-pressure curve follows the methane vapor pressure relationship up to the tropopause. (Both saturated and dry adiabats are shown.) The minimum atmospheric temperature occurs at the tropopause. The range of possible values

for this temperature is between the minimum observed brightness temperature, 80K (at 34 μm), and the minimum value consistent with associated physical parameters, 72K (skin temperature, $T = 2^{-1/4}$ Te). For this model the temperature is 78K and pressure is 10mb, the vapor pressure of CH_4 at 78K. Clouds may form near the tropopause of Titan.

The temperature in the stratosphere increases with increasing altitude, rising to 160 K. The heat source in the stratosphere is attributed to an ultraviolet absorbing dust as in Caldwell's model. At greater heights in the stratosphere, the temperature could remain constant or decrease if the mixing ratio of the dust to other constituents of the atmosphere decreased with height; the temperature is arbitrarily shown constant in figure 2.

The mesopause is at 10^{-5} mb. This is consistent with Strobel's calculation in 1953 (ref. 55) which is based on heat transfer for a solar composition corrected for the larger proportion of CH_4 on Titan. Hunten arbitrarily selected the temperature at the mesopause as 100 K. The temperature in the thermosphere rises gradually with altitude to the base of the exosphere; the range is about 10 K, based on arguments by Strobel (ref. 10). The torus of hydrogen surrounding Saturn is considred an outer exosphere (sec. 2.6). This region will not be in equilibrium with the rest of the atmosphere, and temperatures will be several hundred degrees K because of solar heating.

2.2.5.3 "New" Model

A new model atmosphere has been constructed to incorporate recent information and to use for construction of engineering models for the monograph. The new model is plotted in figure 2, and its parameters are given in table 2. The parameters bracket the Caldwell and Hunten models. The new model adapts the simple atmospheric structure of the temperature inversion model to conform to findings by Owen and Cess (ref. 21) and Lutz et al. (ref 23) that surface pressure is approximately 400 mb and methane abundance is 0.08 km Agt (sec. 2.2.2). N_2 is assumed to be the major constituent on the basis of Hunten's arguments (ref. 9).*

Calculation of the pressure at the inversion based is based on the abundance of gas required to produce the observed geometric albedo $p_v = 0.04$ at 0.26 μm by Rayleigh scattering from a gas overlying a black surface (ref. 27).* If 0.12 km Agt of N_2 were above a strong UV absorber, it would give the observed albedo and produce a pressure of 1.9 mb at the inversion base.

2.2.6 Engineering Models of Titan's Atmosphere

In light of recent information, the main uncertainty in constructing a set of model atmospheres for Titan is whether the atmosphere is deep, i.e., observed features result from opaque clouds that overlie additional atmosphere undetected by infrared

*Danielson's results were scaled to be consistent with a radius of R_a = 2900 km.

observations or whether the atmosphere is thin, i.e., the features result from the surface or absorbing dust in the stratosphere. Consequently, Thick, Thin, and Nominal models are presented in this section. They describe Titan's atmosphere and bracket the extremes of atmospheric parameters given in table 2. The nominal values of Titan's physical parameters specified in table 4 are adopted for all three models. Table 5 gives the compositions, figure 4 shows the pressure-temperature profiles, and figure 5 the altitude-temperature profiles for the three models. The models reflect the following major characteristics: the relative certainty of a stratospheric temperature close to 160 K, the uncertainty in the pressure (altitude) at the base of the temperature inversion, the uncertainty in the total abundances of the atmospheric constituents with consequent uncertainty in the mean molecular weight and surface pressure, and the uncertainty as to whether the thermal structure is governed by the greenhouse or temperature inversion process with consequent uncertainty in the surface temperature.

The Nominal model, which is represented by a solid line in figures 4 and 5, is identical to the new model developed in section 2.2.5.3. The total N_2 abundance of 25 km Agt and the CH_4 abundance of 0.08 km Agt gives a value of 28 for u. The temperature and pressure at the base of the temperature inversion are 160 K and 1.9×10^2 N/m^2. Above the inversion base the temperature remains isothermal. Below the inversion base the temperature decreases to 78 K at the surface where the pressure is 4×10^4 N/m^2. At this temperature the CH_4 in the atmosphere is not saturated.

The Thin atmospheric model is based on the minimum atmospheric abundance and surface temperature that are consistent with observations. This model is represented by an alternating dot-dash line in figures 4 and 5. It is similar to Caldwell's model (sec. 2.2.5.1) but modified to give 0.12 km Agt CH_4 above the inversion base; it closely resembles the nominal model except that it is composed of pure CH_4 and therefore has a value of 16 for u. Accordingly, the temperature and pressure are 1.1×10^2 N/m^2 and 160 K at the inversion base and 1.7×10^3 N/m^2 and 78 K at the surface.

The Thick model is based on the maximum atmospheric abundance and surface temperature that are compatible with current knowledge of Titan. It is shown as a dashed line in figures 4 and 5. The abundances of the major atmospheric constituents are 60 km Agt of N_2 and 0.19 km Agt of CH_4. Therefore, u equals 28 and the surface pressure is 10^5 N/m^2. A weak CH_4 greenhouse effect results in an elevated surface temperature of 125 K. Above the surface the temperature decreases to 76 K at 1.8×10^3 N/m^2 at the tropopause. The remainder of the model, including stratosphere, mesophere, and thermosphere, follows the model of Hunten except as modified to reflect N_2 as the major atmospheric component (sec. 2.2.5.2).

Because the partial pressure of methane in the Thick model is too low to cause cloud formation, Titan's photometric properties must result from non-gaseous atmospheric constituents (sec. 2.3). If the mixing ratio of methane is increased so that $f \geqslant 0.6$, clouds will form near the tropopause (sec.2.3) and the pressure-temperature profile will lie between the profile labeled "thick" in figure 4 and the profile for pure CH_4 labeled "Hunten" in figure 2.

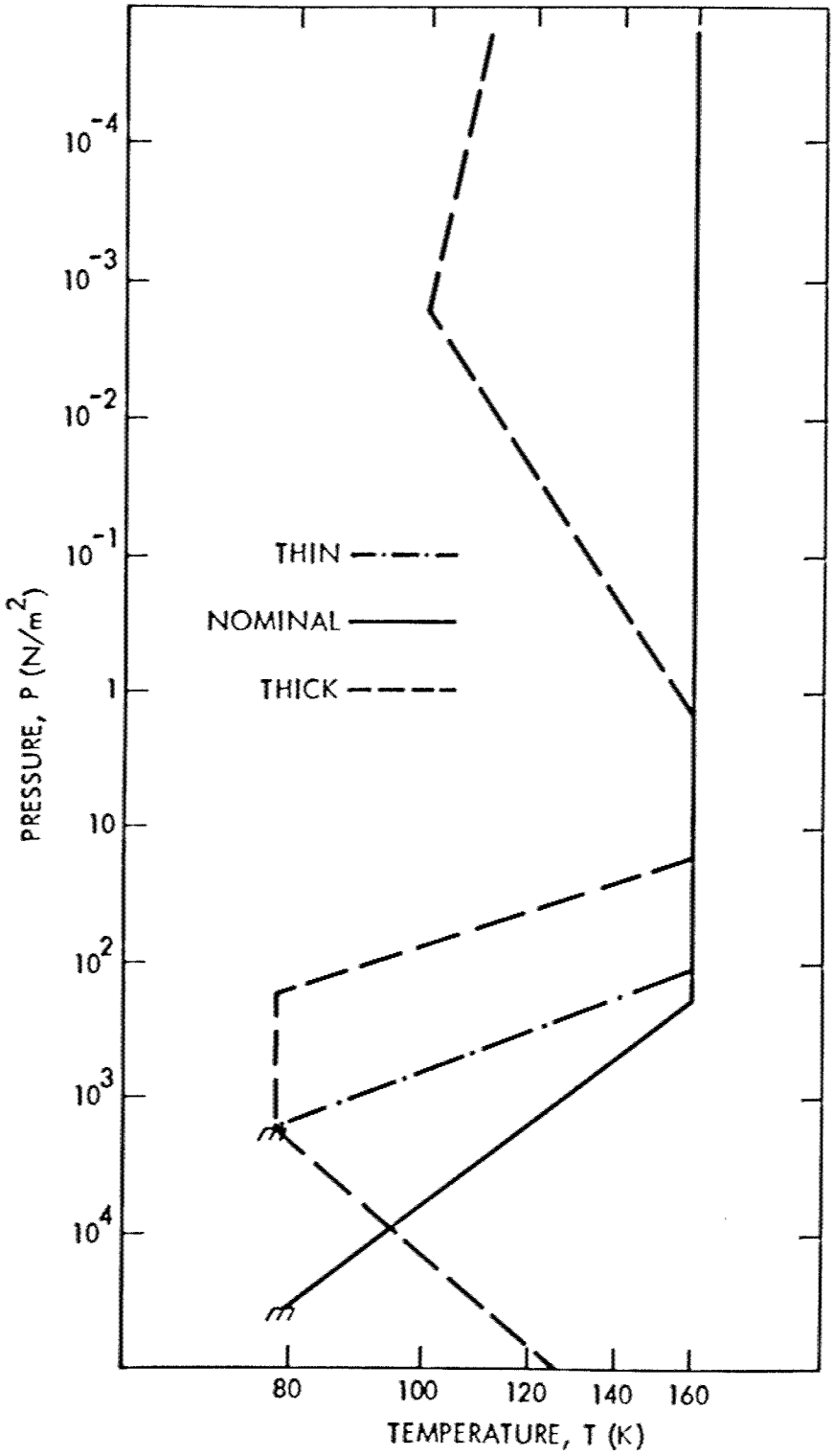

Figure 4. Pressure-Temperature Profiles of Engineering Models of Titan's Atmosphere

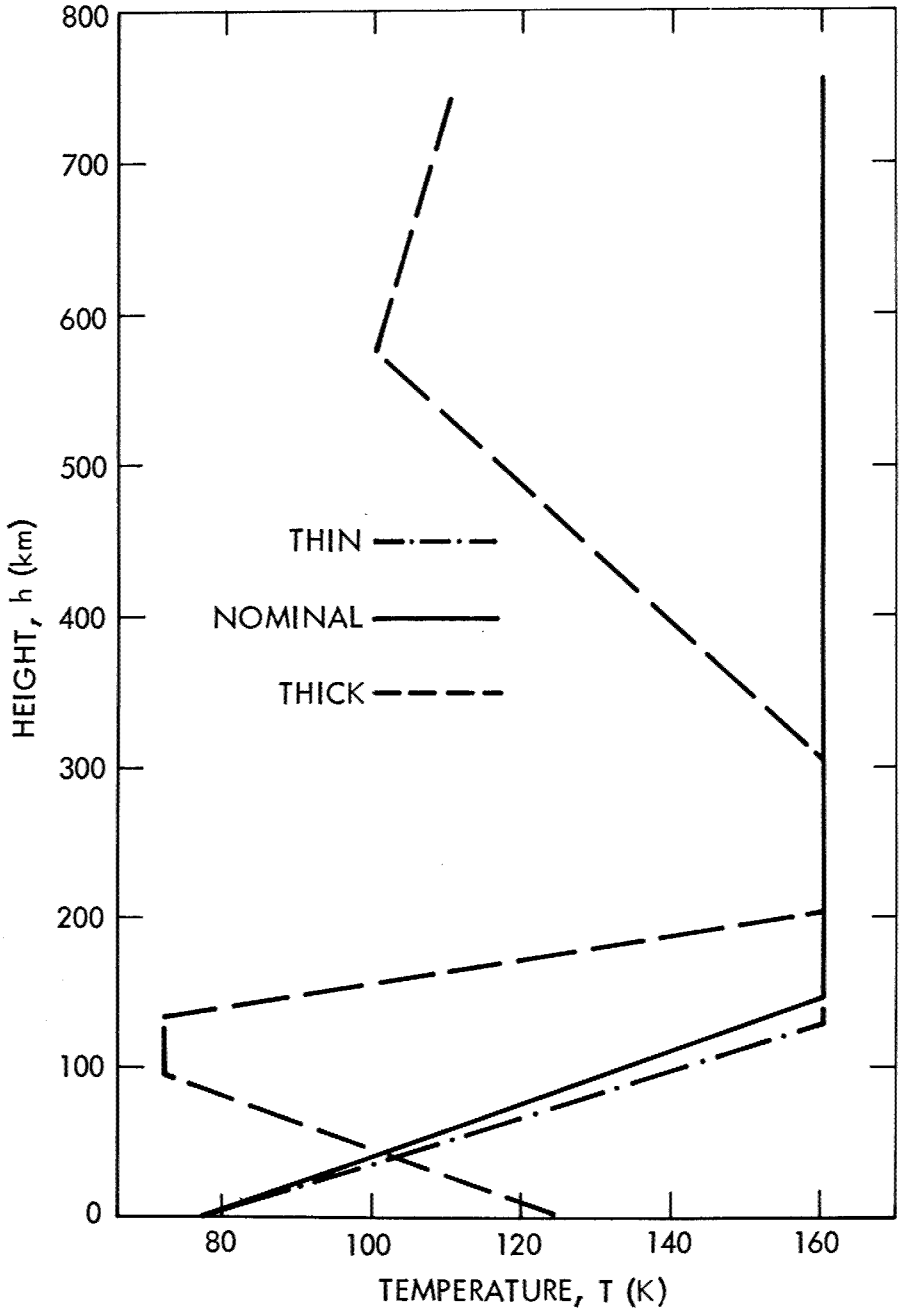

Figure 5. Altitude-Temperature Profiles of Engineering Models of Titan's Atmosphere

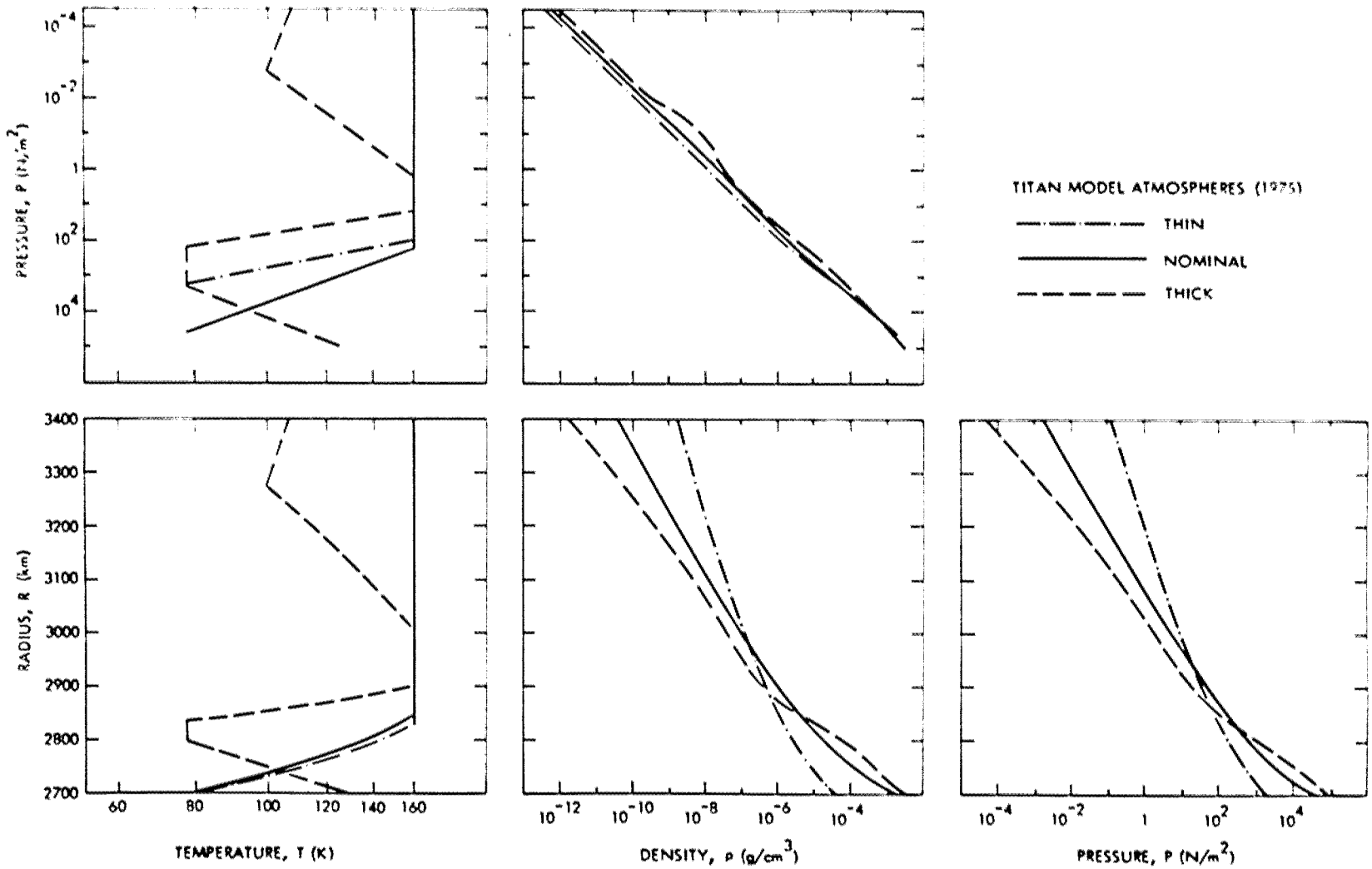

Figure 6. Profiles of Radius, Temperature, Pressure and Density for Engineering Models of Titan's Atmosphere

Profiles of pressure P, temperature T, density ρ, pressure scale height H, geopotential altitude Z, distance R from Titan's center, and molecular number density n for all three models are tabulated in tables 5 through 7. Figure 6 gives the profiles. For all models, zeroes of geopotential altitude Z and physical altitude h correspond to a Titan surface radius of R_s = 2700 km.

2.3 Non-Gaseous Constituents

2.3.1 Aerosols and Dust

Two circumstances suggest the presence of solid condensates such as aerosols or dust in Titan's atmosphere. One is the evidence for the formation of hydrocarbons in methane-rich environments subjected to (solar) UV and electrical discharge (refs. 51, 10, and 55). The other is the low albedo of Titan in the visible and UV portions of the spectrum (sec. 2.2.2). The low albedo indicates the presence of an absorbing substance with reflectivity much smaller than would be expected from a pure cloud or icy surface at the effective reflecting level. These circumstances are consistent with contamination of clouds or surfaces with dust or tar and with suspension of fine dust particles within the atmosphere.

2.3.2 Clouds

There is evidence of clouds in the atmosphere, but it is inconclusive (sec. 2.2.2). Condensation of gases occurs in the lower atmosphere if two conditions are satisfied. (1) The temperature increases with increasing pressure ($dT/dP > 0$) and decreasing altitude ($dT/dZ < 0$) and (2) the partial pressure (fP) of a particular gas exceeds its vapor pressure at the local temperature. (The partial pressure of a gas with mixing ratio f is fP.) Cloud formation is not compatible with condition 1 in the Thin and Nominal models because of the temperature inversion. In the Thick model NH_3 and H_2O clouds cannot form as they are effectively frozen out of the atmosphere. CH_4 clouds are also incompatible with the Thick model because the mixing ratio and thus the partial pressure of CH_4 are so low. In the Thick model, $f = 3.2 \times 10^{-3}$ and the CH_4 partial pressure at the tropopause is only about 6 N/m^2. The vapor pressure of CH_4 at the tropopause temperature (76 K) is 1.1×10^3 N/m^2.

Although clouds cannot form in the atmospheres represented by the engineering models, some observations of Titan can be interpreted to indicate presence of clouds (sec. 2.2.2). If the Thick model is modified so that the CH_4 mixing ratio and thus the partial pressure are sufficient, clouds could form at the tropopause. In figure 7, open circles indicate the CH_4 partial pressures. The top circle indicates the partial pressure if N_2 is the major atmospheric constituent; the bottom circle indicates the partial pressure if it is assumed that CH_4 constitutes a significant portion of the atmosphere (f = 0.6). Because the pressure at the tropopause is approximately 1.1×10^3 N/m^2, a mixing ratio of 0.6 gives a partial pressure of 1.1×10^3 N/m^2. Consequently solid CH_4 ice clouds can form near the tropopause. If the mixing ratio exceeds about 0.6 and the surface

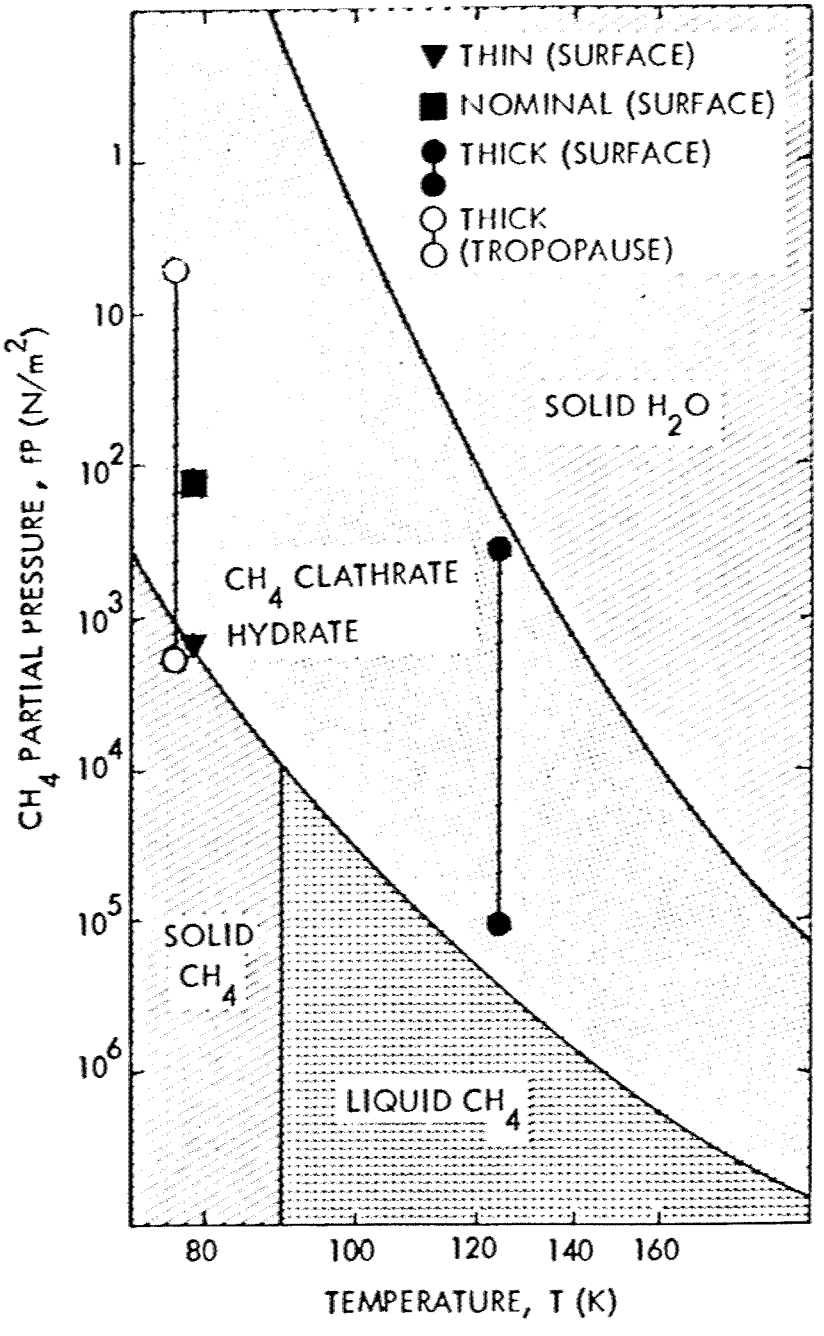

Figure 7. CH_4 Vapor Pressure and CH_4 Clathrate Hydrate Dissociation Pressure Curves Indicating Potential Condensates and Surfaces for the Engineering Models of Titan's Atmosphere.

temperature is lower than that assumed for the extreme model (so the lapse rate (β = (dlogT/dlogP) is less than 0.074), then both CH_4 ice particle clouds and liquid droplet clouds may form within the troposphere, as indicated in figure 7. If clouds form, they probably constitute the primary reflecting or scattering medium for visible sunlight (sec. 2.2.2).

If clouds form, the foregoing solid condensates (sec. 2.3.1) could form nuclei of cloud droplets and associated precipitation, lightning, thunder, and related phenomena might occur. However, Titan's slow rotation and low solar illumination would yield much more subdued weather than on Earth.

2.4 Surfaces

The measured radius of Titan, 2900 km (sec. 2.1.2) is an effective reflecting or absorbing level near an optical depth of unity in the atmosphere. Several candidate surface materials are consistent with the physical chemistry appropriate to the different local conditions which depend on the actual location of the surface below this reflecting level. In particular, the atmospheric pressure must exceed the vapor pressure of the surface material at the local temperature which must be within the stability field of the surface material. The range of the possible temperatures at the surface indicated by microwave radiometric measurements at 8085 MHz is 100 ±30K (sec. 2.2.4). The candidate materials should also be consistent with the likely bulk composition of Titan and its atmosphere (refs. 1, 40, and 56); the materials are given in table 4 and figure 7.

The Nominal model atmosphere is incompatible with either a liquid or solid CH_4 surface. At the surface the temperature is 78 K and the CH_4 partial pressure is 1.3×10^2 N/m^2 as indicated by the square in figure 7. A methane surface would not be stable but would evaporate until the CH_4 was exhausted or equilibrium was established; both possibilities result in more than 0.08 km Agt CH_4 in the atmosphere. Therefore, the surface associated with the Nominal model is most likely solid H_2O or clathrate hydrates of CH_4 and NH_3.

The Thin model atmosphere is compatible with a solid surface of CH_4 because the pure CH_4 atmosphere is saturated (indicated by the triangle in figure 7). The surface could also be NH_3 and CH_4 clathrate hydrates if there is not an excess of CH_4 to condense out of the atmosphere. The 78 K surface temperature is too low for liquid CH_4 to exist.

Figure 7 shows that the Thick model, like the Nominal model, is incompatible with either a liquid or solid CH_4 surface. The two solid circles connected by a line represent the surface conditions for the Thick model (top) and for the model modified with a 0.6 CH_4 mixing ratio (bottom). Conditions for CH_4 abundances between these values fall on the line connecting the points (sec. 2.3). Because of the high surface temperature (T = 125 K) and low mixing ratio ($f \leqslant 0.6$) assumed in this model, the surface is most likely composed of solid H_2O or clathrate hydrates of CH_4 and NH_3.

Although the engineering models do not include a liquid CH_4 surface, such a surface cannot be excluded by observations. If the Thick model atmosphere has a relatively large CH_4 mixing ratio ($f \sim 0.6$) and the surface temperature is not as high as was assumed for the extreme model ($\lesssim$ 115K), then a liquid surface is possible (fig. 7). However, the limited range of necessary conditions make a liquid CH_4 surface unlikely.

Surface deposits of less volatile materials are likely if the surface is solid. A surface at least partly covered with dust or tar is probable because of likelihood of meteorite infall and hydrocarbon production (sec. 2.3).

Some surface activity is to be expected. If the surface is liquid, interactions with atmospheric weather activity (sec. 2.5) may occur although the slow rotation should make this activity much more subdued than for Earth. If the surface is a solid ice crust, thermal stresses within the underlying liquid mantle and release of gravitational energy by collapse may produce ice quakes. Consequently, volcanism and seepages may occur that involve water, steam, and ammonia.

2.5 Temperature Variations and Atmospheric Dynamics

Temperature variations and winds are probably very subdued on Titan. Substantial energy transport and deposition can probably be achieved with modest atmospheric circulation and temperature gradients because of latent heat associated with condensation and vaporization of methane, an important atmospheric constituent (ref. 26). Also a weak symmetric circulation regime is anticipated because of rotation and associated times for thermal transport and relaxation (refs. 57, 58, and 59). Therefore, the horizontal temperature contrasts near the surface are small even between the subsolar point and the current winter pole (a few tenths of a degree Kelvin). Horizontal wind speeds are probably less than 1 m/s, and vertical wind speeds are comparable.

2.6 Upper Atmosphere and Ionosphere

There are no observational data of the upper atmosphere. Theoretical models (refs. 10 and 60) show dominance of molecular hydrogen above the turbopause and provide profiles of H_2 and atomic hydrogen produced by photodissociation.

A torus of hydrogen molecules may surround Saturn because most hydrogen molecules that can escape Titan do not have enough energy to escape Saturn. A theoretical model by McDonough and Brice (ref. 8) predicts that these molecules orbit Saturn until they are lost by photoionization or recaptured in Titan's atmosphere. The model occupies approximately a region on the ecliptic plane that lies between 8 and 60 Saturn radii distant from Saturn. It has a thickness that extends about 5 Saturn radii on each side of Titan's orbital plane. The predicted torus has a molecular or atomic density of 1 to 10^3 cm^{-3}; it is an extension of and is in equilibrium with Titan's exosphere.

Whitten et al. (ref. 12) have estimated ionospheric densities and temperatures from models of the upper atmosphere, solar ultraviolet flux, and reaction rates for the competing processes of ionization, dissociation and recombination. The estimates indicate a maximum electron density of (0.7 to 4) $\times 10^3$ cm^{-3} that occurs between altitudes of 1000 and 3000 km with electron and hydrogen ion temperatures of approximately 200 to 400 K. The location of the peak corresponds to H_2 concentrations of 10^9 to 10^{10} cm^{-3}.

Lower in the atmosphere ionization by galactic cosmic rays may be significant. Capone et al. (ref. 13) have estimated that ion and electron concentrations may exceed 10^3 cm^{-3} at an altitude where the concentration of neutral molecules is about 10^{18} cm^{-3} (tables 5 through 7). The dominant ions, which result from the ion chemistry in this region of high molecular concentration, are probably $C^3H_{11}^+$, $C^2H_9^+$, and $C^3H_9^+$.

3. CRITERIA

The criteria section provides a description of the environment of Titan intended for use in design and mission planning for orbiters, probes, and landers. Essential data pertaining to Saturn is available in The Planet Saturn (1970) (NASA SP-8091). The environment described here is based on results of investigations discussed in the State-of-the-Art section. Uncertainty estimates or limiting values represent the extreme range of possible values to be used for design. The real environment of Titan, however, will probably contain some surprises.

3.1 Physical Data

Values and uncertainties of radius, mass, mean density, and other physical, astronomical and orbital data are specified in table 3. The table does not include oblateness, magnetic field, and trapped radiation which are presently unknown. The symbols used are listed and defined in appendix B. Some terms employed in this monograph are defined in appendix C.

The rotation of Titan is synchronous with its revolution about Saturn and its pole perpendicular to its orbit. The rotational rate, period, and inclination in table 3 reflect these assumptions.

3.2 Model Atmospheres

Table 4 specifies compositions, molecular weights, and other parameters for Thin, Nominal, and Thick model atmospheres which represent the extreme and nominal values of the atmospheric parameters. The profiles of pressure P, temperature T, density ρ, pressure scale height H, geopotential altitude Z, distance R from Titan's center, and molecular number density n are presented in tables 5 through 7 and in figure 6. Although in some regions the pressure-temperature profiles for the different models are

Table 3
Physical Parameters for Titan

Parameter	Value
Radius (Surface) (Atmosphere)	$R_s = 2700 \pm 200$ km $R_a = 2900 \pm 100$ km
Mass	$M = (1.37 \pm 0.02) \times 10^{23}$ kg
Mean Density	$\bar{\rho} = 1.7 \pm 0.4$ g/cm^3
Acceleration of Gravity at Surface	$g_o = 1.3 \pm 0.2$ m/s^2
Escape Speed	$V_e = 2.6 \pm 0.1$ km/s
Visual Geometric Albedo	$p_v = 0.15 \pm 0.03$
Bolometric Bond Albedo	$A_{bol} = 0.20 + 0.03$
Effective Temperature	$T_e = 85 \pm 2$ K
Rotation	$\omega = 4.56 \times 10^{-6}$ s^{-1}
Period of Rotation (Earth day)	15.945 days
Inclination of Equator to Ecliptic Plane	26°.7
Period of Revolution about Sun (Earth)	29.46 yr
Distance from Sun	9.0 to 10.1 AU

identical. other properties, e.g., molecular number densities, are not necessarily identical and the appropriate tables or graph should be consulted for the required information.

3.3 Non-Gaseous Constituents

Probable non-gaseous atmospheric constituents for the three model atmospheres are given in table 4. Meteoritic dust and various hydrocarbons, both dark absorbers, probably occur as fine particles which may be suspended in the atmosphere or cover the surface. The particles apparently modify the photometric and polarimetric properties of Titan because observations of these properties differ from those made of either a pure gaseous atmosphere or a typical planetary surface (secs. 2.2.2 and 2.3). The effective reflecting layer in the visible spectrum is probably 200 or 300 km above the actual surface.

Table 4
Compositions and Parameters for Model Atmospheres, Condensates, and Surfaces of Titan

Model	Abundances of Major Constituents and Molecular Weights	Ratio $\mu m_H/k$ $\left(\frac{g}{cm^3}\ \frac{K}{N/m^2}\right)$	Ratio $k/\mu m_H g_o$ (km/K)	Condensates	Surface
Thin	1.6 km Agt CH_4 u = 16 g/mole	1.936×10^{-6}	0.3973	hydrocarbon polymers	Solid: CH_4, H_2O or clathrate hydrates of NH_3 and CH_4
Nominal	25 km Agt N_2 0.08 km Agt CH_4 u = 28 g/mole	3.388×10^{-6}	0.2270	hydrocarbon polymers	Solid: H_2O or clathrate hydrates of NH_3 and CH_4
Thick	60 km Agt N_2 $\geqslant$0.19 km Agt CH_4 u = 28 g/mole*	3.388×10^{-6}	0.2270	hydrocarbon polymers*	Solid: H_2O or clathrate hydrates of NH_3 and CH_4*

*If the CH_4 mixing ratio $f \gtrsim 0.6$ additional condensate and surface species (i.e. solid or liquid CH_4) are possible; see sections 2.2.6, 2.3, and 2.4.

Table 5*
Thin Model Atmosphere of Titan

P (N/m^2)	T (K)	ρ (g/cm^3)	H (km)	Z (km)	R (km)	n (cm^{-3})
1.0(-5)	160	1.2(-13)	194	1155	4717	4.5(9)
1.0(-4)	160	1.2(-12)	162	1008	4309	4.5(10)
1.0(-3)	160	1.2(-11)	137	862	3965	4.5(11)
1.0(-2)	160	1.2(-10)	118	716	3673	4.5(12)
1.0(-1)	160	1.2(-9)	102	569	3421	4.5(13)
1.0	160	1.2(-8)	89	423	3201	4.5(14)
2.0	160	2.4(-8)	86	379	3141	9.1(14)
5.0	160	6.0(-8)	82	320	3064	2.3(15)
10	160	1.2(-7)	79	276	3008	4.5(15)
20	160	2.4(-7)	76	232	2954	9.1(15)
50	160	6.0(-7)	73	174	2886	2.3(16)
1.1(2)	160	1.3(-6)	70	124	2830	5.0(16)
2.0(2)	137	2.8(-6)	58	89	2792	1.1(17)
5.0(2)	108	9.0(-6)	44	45	2745	3.4(17)
1.0(3)	90	2.1(-5)	36	18	2718	8.1(17)
1.4(3)	82	3.3(-5)	33	6	2706	1.2(18)
1.7(3)	78	4.2(-5)	31	0	2700	1.6(18)

*Numbers in parentheses are powers of ten.

Solid or liquid CH_4 clouds may be present if there are elevated surface temperatures (90 to 124 K) as well as large methane mixing ratios ($f \geqslant 0.6$). These conditions are indicated on figure 7. If clouds are present, they probably form the visual reflecting layer 200 or 300 km above the actual surface. Also, precipitation is possible if clouds are present.

3.4 Surfaces

Several candidate surfaces are possible. However, CH_4 and NH_3 clathrate hydrates are the most likely in the observed temperature, pressure, and abundance ranges. Solid water ice, solid methane, and liquid methane are also possible. The candidate surface materials and necessary conditions are shown in table 4 and figure 7. Any surface may be strongly contaminated with meteoric dust and hydrocarbon deposits. Geological activity may produce ice-quakes that cause volcanism and seepages that are dominated by water, steam, and ammonia.

Table 6*
Nominal Model Atmosphere of Titan

P (N/m^2)	T (K)	ρ (g/cm^3)	H (km)	Z (km)	R (km)	n (cm^{-3})
1.0(-5)	160	2.1(-13)	69.5	748	3734	4.5(9)
1.0(-4)	160	2.1(-12)	63.9	664	3581	4.5(10)
1.0(-3)	160	2.1(-11)	58.9)	580	3439	4.5(11)
1.0(-2)	160	2.1(-10)	54.6	497	3309	4.5(12)
2.0(-2)	160	4.2(-10)	53.3	472	3272	9.1(12)
5.0(-2)	160	1.1(-9)	51.8	438	3223	2.3(13)
1(-1)	160	2.1(-9)	50.6	413	3188	4.5(13)
2(-1)	160	4.2(-9)	49.5	388	3153	9.1(13)
5(-1)	160	1.1(-8)	48.1	354	3108	2.3(14)
1.0	160	2.1(-8)	47.1	330	3075	4.5(14)
2.0	160	4.2(-8)	46.1	304	3043	9.1(14)
5.0	160	1.1(-7)	44.9	271	3001	2.3(15)
10	160	2.1(-7)	44.0	246	2971	4.5(15)
20	160	4.2(-7)	43.1	221	2940	9.1(14)
50	160	1.1(-6)	41.9	187	2901	2.3(16)
1.0(2)	160	2.1(-6)	41.1	162	2873	4.5(16)
1.9(2)	160	4.0(-6)	40.4	139	2846	8.6(16)
2.0(2)	159	4.3(-6)	40.0	137	2844	9.1(16)
5.0(2)	141	1.2(-5)	34.5	106	2810	2.6(17)
1.0(3)	128	2.6(-5)	31.0	84	2787	5.7(17)
2.0(3)	117	5.8(-5)	27.8	65	2767	1.2(18)
5.0(3)	103	1.6(-4)	24.2	42	2743	3.5(18)
1.0(4)	94	3.6(-4)	21.8	27	2727	7.7(18)
2.0(4)	86	7.9(-4)	19.6	13	2713	1.7(19)
4.0(4)	78	1.7(-3)	17.7	0	2700	3.7(19)

*Numbers in parentheses are powers of ten.

Table 7*
Thick Model Atmosphere of Titan

P (N/m^2)	T (K)	ρ (g/cm^3)	H (km)	Z (km)	R (km)	n (cm^{-3})
1.8(-5)	110	5.4(-13)	40.6	583	3443	1.2(10)
3.0(-5)	109	9.3(-13)	39.7	569	3421	2.0(10)
1.0(-4)	106	3.2(-12)	37.6	540	3375	6.8(10)
3.0(-4)	104	9.8(-12)	35.9	514	3335	2.1(11)
1.0(-3)	101	3.4(-11)	34.1	486	3292	7.2(11)
1.8(-3)	100	5.9(-11)	33.4	473	3273	1.3(12)
3.0(-3)	104	9.8(-11)	34.2	461	3256	2.1(12)
1.0(-2)	113	3.0(-10)	36.2	431	3213	6.4(12)
3.0(-2)	121	8.4(-10)	38.0	402	3172	1.8(13)
1.0(-1)	132	2.6(-9)	40.0	367	3125	5.5(13)
3.0(-1)	142	7.2(-9)	41.9	333	3080	1.5(14)
1.0	154	2.2(-8)	44.0	293	3028	4.7(14)
1.8	160	3.7(-8)	44.9	273	3003	7.9(14)
2.0	160	4.2(-8)	44.8	268	2997	9.1(14)
5.0	160	1.1(-7)	43.6	235	2957	2.3(15)
10	160	2.1(-7)	42.7	209	2927	4.5(15)
18	160	3.7(-7)	42.0	189	2903	7.9(15)
20	153	4.4(-7)	40.1	184	2898	9.5(15)
50	124	1.5(-6)	29.1	157	2866	3.2(16)
1.0(2)	91	3.7(-6)	23.0	141	2848	8.0(16)
1.8(2)	76	7.8(-6)	19.0	130	2837	1.7(17)
2.0(2)	76	8.9(-6)	19.0	128	2834	1.9(17)
5.0(2)	76	2.2(-5)	18.8	112	2817	4.8(17)
1.0(3)	76	4.5(-5)	18.6	100	2804	9.5(17)
1.8(3)	76	7.8(-5)	18.5	90	2794	1.7(18)
3.0(3)	81	1.3(-4)	19.6	81	2783	2.7(18)
1.0(4)	94	3.6(-4)	22.3	57	2758	7.7(18)
3.0(4)	108	9.4(-4)	25.1	32	2732	2.0(19)
1.0(5)	125	2.7(-3)	28.4	0	2700	5.8(19)

*Numbers in parentheses are powers of ten.

3.5 Temperature Variations and Atmospheric Dynamics

Horizontal and temporal variations in temperature in the atmosphere and at the surface do not exceed a few tenths of a degree Kelvin. The warmest region corresponds to the subsolar point and the coolest to the winter pole. A symmetric regime dominates atmospheric circulation, but both horizontal and vertical wind speeds are less than 1 m/s. Weather is possible including precipitation and electrical discharge that would be much more subdued and less frequent than on Earth.

3.6 Upper Atmosphere and Ionosphere

There may be a torus of molecular or atomic hydrogen surrounding Saturn which occupies approximately the region between 8 and 80 Saturn radii distant from Saturn and has a thickness of 10 Saturn radii that extends 5 Saturn radii on each side of Titan's orbital plane. The particle density within the torus would be about 10^3 cm^{-3}. The torus would be an extension of Titan's exosphere.

The maximum electron density in Titan's ionosphere may be of the order of 4×10^3 cm^{-3} with temperatures of approximately 400 K. The maximum would occur at an altitude of about 2000 km which corresponds to a H_2 concentration of 10^9 to 10^{10} cm^{-3}. Lower in the atmosphere a second maximum may occur. Electron densities at an altitude which corresponds to a molecular density of approximately 10^{18} cm^{-3} (tables 5 through 7) may be of the order of 10^3 cm^{-3}. The electrons would be in thermal equilibrium with the atmosphere.

REFERENCES

1. Lewis, J. S.: Satellites of the Outer Planets: Their Physical and Chemical Nature. Icarus, Vol. 15, No. 2, 1971, pp. 174-185.

2. Morrison, D.: Radius and Mass of Titan. The Atmosphere of Titan. NASA SP-340, 1974, pp. 9-11.

3. Hunten, D. M., editor: The Atmosphere of Titan. NASA SP-340, 1974.

4. Elliot, J. L.; Veverka, J.; Goguen, J.; and Dunham, T.: The Albedo Distribution Across Titan's Disk. Bull. Amer. Astron. Soc., Vol. 7, No. 2., 1975, p. 384.

5. McGovern, W. E.: Upper Limit of Hydrogen and Helium Concentrations on Titan. Planetary Atmospheres, C. Sagan; T. C. Owen; and H. J. Smith, eds. I.A.U. Symposium No. 40, D. Reidel Publishing Company, Dordrecht, Holland, 1971, pp. 394-400.

6. Hunten, D. M.: The Escape of H_2 from Titan. J. Atm. Sci., Vol. 30, No. 4, 1973, pp. 726-732.

7. Gross, S. H.: The Atmospheres of Titan and the Galilean Satellites. J. Atm. Sci., Vol. 31, No. 5, 1974, pp. 1413-1420.

8. McDonough, T. R.; and Brice, N. M.: A Saturnian Gas Ring and the Recycling of Titan's Atmosphere. Icarus, Vol. 20, No. 2, 1973, pp. 136-145.

9. Hunten, D. M.: Titan's Atmosphere and Surface. Proceedings I.A.U. Colloquium No. 28, Planetary Satellites, 18-21 August 1974, Ithaca, New York. To be published, University of Arizona Press, 1975.

10. Strobel, D. F.: The Photochemistry of Hydrocarbons in the Atmosphere of Titan. Icarus, Vol. 21, No. 4, 1974, pp. 466-470.

11. Strobel, D. F.: Aeronomy of the Major Planets: Photochemistry of Ammonia and Hydrocarbons. A.G.U. Trans. EOS, Vol. 56, No. 2, 1975, p. 141.

12. Whitten, R. C.; McCulley, L.; and Michelson, P. F.: The Upper Ionosphere of Titan. A.G.U. Trans. EOS, Vol. 56, No. 6, 1975, p. 406.

13. Capone, L. A.; Whitten, R. C.; Dubach, J.; Prasad, S. S.; and Huntress, Jr., W. T.: The Lower Ionosphere of Titan. To be published in 1975.

14. Barker, E. S.; and Trafton, L. M.: Ultraviolet Reflectivity and Geometrical Albedo of Titan. Icarus, Vol. 20, No. 4, 1973, pp. 444-454.

15. Caldwell, John: Thermal Radiation from Titan's Atmosphere. Proceedings I.A.U. Colloquium No. 28, Planetary Satellites, 18-21 August 1974, Ithaca, New York. To be published, University of Arizona Press, 1975.

16. McCord, T. B.; Johnson, T. V.; and Elias, J. H.: Saturn and its Satellites: Narrow-Band Spectrophotometry (0.3-1.1 μ). Astrophys. J., Vol. 165, No. 2, 1971, pp. 413-424.

17. Younkin, R. L.: The Albedo of Titan. Icarus, Vol. 21, No. 4, 1974, pp. 219-229.

18. Nolan, M.; Veverka, J.; Morrison, D.; Cruikshank, D. P.; Lazarewicz, A.; Morrison, N. D.; Elliot, J. L.; Goguen, J.; and Burns, J.: Six-Color Photometry of Iapetus, Titan, Rhea, Dione, and Tethys. Icarus, Vol. 23, No. 3, 1974, pp. 334-354.

19. Harris, D. L.: Photometry and Colorimetry of Planets and Satellites. Planets and Satellites, G. P. Kuiper and B. M. Middlehurst, eds. University of Chicago Press, 1961, pp. 272-342.

20. Johnson, T. V.; and Pilcher, C. B.: Review of Satellite Spectrophotometry and Composition. Proceedings I.A.U. Colloquium No. 28, Planetary Satellites, 18-21 August 1974, Ithaca, New York. To be published, University of Arizona Press, 1975.

21. Owen, T.; and Cess, R. D.: Methane Absorption in the Visible Spectra of the Outer Planets and Titan. Astrophys. J., Vol. 197, No. 1, 1975, pp. L37-40.

22. Owen, T. C.: Personal Communication, 1975.

23. Lutz, B. L.; Owen, T.; and Cess, R. D.: Laboratory Band Strengths of Methane and Their Application to the Atmospheres of Jupiter, Saturn, Uranus, Neptune and Titan. Astrophys. J. To be published in 1975.

24. Cess, R.; and Owen, T.: The Effect of Noble Gases on an Atmospheric Greenhouse (Titan). Nature, Vol. 244, 1973, pp. 272-273.

25. Encrenaz, Th.; Owen, T.; Woodman, J. H.: The Abundance of Ammonia on Jupiter, Saturn and Titan. Astron. & Astrophys., Vol. 37, No. 1, 1974, pp. 49-55.

26. Danielson, R. E.; Caldwell, J. J.; and Larach, D. R.: An Inversion in the Atmosphere of Titan. Icarus, Vol. 20, No. 4, 1973, pp. 437-443.

27. Danielson, R. E.; Caldwell, J. J.; and Larach, D. R.: An Inversion in the Atmosphere of Titan. The Atmosphere of Titan. NASA SP-340, 1974, pp. 92-109.

28. Caldwell, J.; Larach, D. R.; and Danielson, R. E.: The Continuum Albedo of Titan. Bull. Amer. Astron. Soc., Vol. 5, No. 2, 1973, p. 305.

29. Caldwell, J.: Ultraviolet Observations of Small Bodies in the Solar System by OAO-2. Icarus, Vol. 25, No. 3, 1975, pp. 384-396.

30. Nolan, M.; and Veverka, J.: The Phase Coefficient of Titan. Bull. Amer. Astron. Soc., Vol. 6, No. 3, 1974, pp. 386-387.

31. Veverka, J.: Photometry and Polarimetry of Satellite Surfaces. Proceedings I.A.U. Colloquium No. 28, Planetary Satellites, 18-21 August 1974, Ithaca, New York. To be published. University of Arizona Press, 1975.

32. Veverka, J.: Titan: Polarimetric Evidence for an Optically Thick Atmosphere? Icarus, Vol. 18, No. 4, 1973, pp. 657-660.

33. Zellner, B.: The Polorization of Titan. Icarus, Vol. 18, No. 4, 1973, pp. 661-664.

34. Noland, M.; Veverka, J.; and Goguen, J.: New Evidence for the Variability of Titan. Astrophys. J., Vol. 194, No. 3, 1974, pp. L157-158.

35. Andersson, L.: Variability of Titan – 1896-1974. To be published in 1975.

36. Lockwood, G. W.: The Secular and Orbital Brightness Variations of Titan, 1972-1974. Astrophys. J., Vol. 195, No. 3, 1975, pp. L137-139.

37. Kuiper, G. P.: Titan: A Satellite with an Atmosphere. Astrophys. J., Vol. 100, 1944, pp. 378-383.

38. Kuiper, G. P.: Planetary Atmospheres and their Origin. The Atmospheres of the Earth and Planets, G. P. Kuiper, ed., University of Chicago Press, 1952, pp. 306-405.

39. Trafton, L.: On the Possible Detection of H_2 in Titan's Atmosphere. Astrophys. J., Vol. 175, No. 1, 1972a, pp. 285-293.

40. Trafton, L.: The Bulk Composition of Titan's Atmosphere. Astrophys. J., Vol. 175, No. 1, 1972b, pp. 295-306.

41. Trafton, L. M.: Near-Infrared Spectrophotometry of Titan. Icarus, Vol. 24, No. 4, 1975b, pp. 443-453.

42. Gillett, F. C.: Further Observations of the 8-13 Micron Spectrum of Titan. To be published in 1975.

43. Gillett, F. C.; Forrest, W. J.; and Merrill, K. M.: 8-13 Micron Observations of Titan. Astrophys. J., Vol. 184, No. 2, 1974, pp. L93-95.

44. Knacke, R. F.; Owen, T.; and Joyce, R. R.: Infrared Observations of the Surface and Atmosphere of Titan. Icarus, Vol. 24, No. 4, 1975, pp. 460-464.

45. Low, F. J.; and Rieke, G. H.: Infrared Photometry of Titan. Astrophys. J., Vol. 190, No. 3, 1974, pp. L143-145.

46. Joyce, R.; Knacke, R. F.; and Owen, T.: An Upper Limit on the 4.9-Micron Flux from Titan. Astrophys. J., Vol. 183, No. 1, 1973, pp. L31-33.

47. Allen, D. A.; and Murdock, T. L.: Infrared Photometry of Saturn, Titan, and the Rings. Icarus, Vol. 14, No. 1, 1971, pp. 1-2.

48. Morrison, D.; Cruikshank, D. P.; and Murphy, R. E.: Temperatures of Titan and the Galilean Satellites at 20 Microns. Astrophys. J., Vol. 173, No. 3, 1972, pp. L143-146.

49. Pollack, J. B.: Greenhouse Models of the Atmosphere of Titan. Icarus, Vol. 19, No. 1, 1973, pp. 43-58.

50. Fox, K.: Estimates of Quasipolar Absorption by Methane in the Atmosphere of Titan. Icarus, Vol. 24, No. 4, 1975, pp. 454-459.

51. Sagan, C.: The Greenhouse of Titan. Icarus, Vol. 18, No. 4, 1973, pp. 649-656.

52. Briggs, F. H.: The Radio Brightness of Titan. Icarus, Vol. 22, No. 1, 1974, pp. 48-50.

53. Divine, N.: Titan Atmosphere Models (1973). Jet Propulsion Laboratory, TM 33-672.

54. Kessler, W. C.; and Myers, H.: The Effect of Uncertainties in Titan Atmospheric Models on Entry Probe Design and Feasibility. McDonnell Douglas Astronautics-East, Report No. MDC E104.

55. Strobel, D. F.: The Photochemistry of NH_3 in the Jovian Atmosphere. J. Atm. Sci., Vol. 30, No. 6, 1973, pp. 1205-1209.

56. Lewis, J. S.; and Prinn, R. G.: Titan Revisited. Comments on Astrophys. Space Phys., Vol. 5, No. 1, 1973, pp. 1-7.

57. Leovy, C. B.; and Pollack, J. B.: A First Look at Atmospheric Dynamics and Temperature Variations on Titan. Icarus, Vol. 19, No. 2, 1973, pp. 195-201.

58. Leovy, C. B.; and Pollack, J. B.: Further Comment on Titan's Atmospheric Scaling. Icarus, Vol. 24, No. 1, 1975, pp. 76-77.

59. Golitsyn, G. S.: Another Look at Atmospheric Dynamics on Titan and Some of Its General Consequences. Icarus, Vol. 24, No. 1, 1975, pp. 70-75.

60. Tabarie, N.: Distribution of Hydrogen and its Lyman-Alpha Intensity in the Atmosphere of Titan. Icarus, Vol. 23, No. 3, 1974, pp. 363-373.

APPENDIX A

ATMOSPHERIC STRUCTURE RELATIONS

In terms of the symbols defined in Appendix B, the models are governed, within each atmospheric region by the equations which represent

(1) hydrostatic equilibrium $$\frac{dP}{dR} = -\rho g_o \, (R_s/R)^2 \tag{A1}$$

(2) the perfect gas law $$\rho = u m_H P/kT \tag{A2}$$

and (3) a temperature gradient $$\frac{d\log T}{d\log P} = \beta \tag{A3}$$

Substitution of the geopotential altitude, given by $Z = R_s - (R_s^2/R)$ in equal A1 yields solutions of the form

$$T = T_A (P/P_A)^\beta \tag{A4}$$

and

$$Z = Z_A - k(T - T_A)/u m_H g_o \beta \tag{A5}$$

for constant $\beta \neq 0$ in a region within which the values Z_A, P_A, and T_A describe a common level. If $\beta = 0$ equation A5 is replaced by

$$Z = Z_A - (kT_A/u m_H g_o) \, \ell n \, (P/P_A) \tag{A6}$$

The auxiliary quantities pressure scale height, molecular number density and mean molecular weight are given by

$$H = (kT/u m_H g_o) \, (R/R_s)^2 \tag{A7}$$

$$n = P/kT \tag{A8}$$

and $$u = \sum_i f_i m_i / m_H \tag{A9}$$

Here m_i is the mass of a molecule whose mixing ratio (fraction by number or volume) f_i is proportional to its abundance.

APPENDIX B

SYMBOLS

A_{bol}	bolometric Bond albedo of Titan (0.20 ±0.06)
B_λ	black-body radiation intensity for unit wavelength interval ($W\ cm^{-3}\ sr^{-1}$)
f	mixing ratio = fraction by number or volume
g_o	acceleration of gravity at $R = R_a$ (1.3 ±0.2 m/s^2)
h	altitude above surface (km)
H	pressure scale height (km)
k	Boltzmann's constant (1.38×10^{-23} J/K)
m_H	mass of Hydrogen atom (1.6×10^{-27} kg)
M	mass of Titan ([1.37 ±0.02] $\times 10^{23}$ kg)
n	number of molecules per unit volume (cm^{-3})
p_v	visual geometric albedo of Titan (0.15 ±0.03)
P	local pressure of atmospheric gas (N/m^2)
P_A	P evaluated at the level A (N/m^2)
$P(CH_4)$	partial pressure of methane (N/m^2)
R	distance from center of Titan (km)
R_a	radius of Titan's atmosphere (2900 ±100 km)
R_s	radius of Titan's surface (2700 ±200 km)
T	local temperature of atmospheric gas (K)
T_e	effective temperature of Titan (85 ±2 K)
T_A	T evaluated at the level A (K)
u	mean molecular weight of atmospheric gas
V_e	escape speed from Titan (2.6 ±0.1 km/s)
Z	geopotential altitude (km)
Z_A	Z evaluated at the level A (km)
β	logarithmic pressure-temperature gradient
ϵ	thermal radiative emissivity
λ	electromagnetic wavelength (m)
ρ	local mass density of atmospheric gas (g/cm^3)
$\bar{\rho}$	mean density of Titan (1.7 ±0.4 g/cm^3)
ω	rotation rate of Titan ($4.56 \times 10^{-6}\ s^{-1}$)

APPENDIX C

GLOSSARY

amagat (Agt) – The density of an ideal gas at standard temperature and pressure (STP). The product of amagat times length is the abundance of gas in a column with unit area. At STP Avagadro's number N_o of molecules (1 mole) occupies a volume V_o and 1 meter amagat = 1 $m(N_o/V_o) = 2.69 \times 10^{25}$ molecules/m^2.

brightness temperature – The temperature of a black-body which would radiate the same power per unit area as the observed body at the wavelengths under consideration.

bolometric Bond albedo – The ratio of total power reflected from a body to total solar power incident on it.

exosphere – The atmospheric region where a molecule's mean-free-path exceeds its scale height. This region is nearly collision free, and molecules with thermal speed in excess of Titan's escape speed may escape. The exobase or location of the lower boundary of the exosphere is usually in the thermosphere.

geopotential altitude (Z) – The integral of the relative acceleration of gravity g along a radius R, defined by

$$Z = \int_{R_s}^{R} (g/g_o)\,dR.$$

If departures from spherical symmetry and the mass external to a sphere of radius R, both contribute negligibly to g, then $Z = R_s - (R_s^2/R)$. For $|Z| \ll R_s$, the geopotential altitude Z is equivalent to the geometric altitude $(R - R_s)$.

ionosphere – The atmospheric region in which the major maxima of electron and ion concentrations occur. The ionospheric layers usually occur in the mesosphere and thermosphere.

mesopause – The atmospheric level where the temperature, which decreases with altitude in the mesosphere, reaches a minimum. This minimum is caused by the relative absence of any strong heating mechanisms. Above the mesopause the temperature increases in the thermosphere.

mesophere – The region extending from the stratopause to the mesopause. In this region energy deposited in the stratosphere is conducted or radiated upwards causing the temperature to decrease with altitude.

scale height (H) – A measure of the vertical gradient of an atmospheric quantity x (e.g.

pressure P), such that if $H = -x(dx/dR)^{-1}$ is constant with radial distance R, the quantity x changes by a factor e in the interval ($\Delta R = H$).

stratopause – The atmospheric level where the temperature, which increases with altitude in the stratosphere, reaches a local maximum.

stratosphere – The atmospheric region of constant and then increasing temperature extending from the tropopause to the stratopause. Heating is caused by secondary energy transport processes, primarily absorption of solar ultraviolet radiation.

thermosphere – The atmospheric region above the mesopause. Efficient absorption of solar ultraviolet radiation and inefficient conduction and radiation produce high temperatures in this region.

tropopause – The top boundary of the troposphere, characterized by an abrupt change in the decreasing temperature gradient that extends from the surface.

troposphere – The atmospheric region between the surface and the tropopause. Weather occurs in this dense region as a result of major atmospheric energy transport processes. The processes include radiative transfer, convection, advection, condensation, and evaporation. Radiative transfer generally produces a decreasing temperature with increasing altitude.

turbosphere – The portion of the atmosphere that is characterized by turbulence. Turbulent mixing extends from the surface to the turbopause. Above the turbopause turbulent mixing is ineffective and various molecular species may not be in thermal equilibrium.

NASA SPACE VEHICLE DESIGN CRITERIA MONOGRAPHS

ENVIRONMENT

SP-8005	Solar Electromagnetic Radiation, revised May 1971
SP-8010	Models of Mars' Atmosphere (1974) revised December 1974
SP-8011	Models of Venus Atmosphere (1972), revised September 1972
SP-8013	Meteoroid Environment Model–1969 (Near Earth to Lunar Surface), March 1969
SP-8017	Magnetic Fields–Earth and Extraterrestrial, March 1969
SP-8020	Surface Models of Mars (1975), revised September 1975
SP-8021	Models of Earth's Atmosphere (90 to 2500 km), revised March 1973
SP-8023	Lunar Surface Models, May 1969
SP-8037	Assessment and Control of Spacecraft Magnetic Fields, September 1970
SP-8038	Meteoroid Environment Model–1970 (Interplanetary and Planetary), October 1970
SP-8049	The Earth's Ionosphere, March 1971
SP-8067	Earth Albedo and Emitted Radiation, July 1971
SP-8069	The Planet Jupiter (1970), December 1971
SP-8084	Surface Atmospheric Extremes (Launch and Transportation Areas), revised June 1974
SP-8085	The Planet Mercury (1971), March 1972
SP-8091	The Planet Saturn (1970), June 1972
SP-8092	Assessment and Control of Spacecraft Electromagnetic Interference, June 1972

SP-8103	The Planets Uranus, Neptune, and Pluto (1971), November 1972
SP-8105	Spacecraft Thermal Control, May 1973
SP-8111	Assessment and Control of Electrostatic Charges, May 1974
SP-8116	The Earth's Trapped Radiation Belts, March, 1975
SP-8117	Gravity Fields of the Solar System, April 1975
SP-8118	Interplanetary Charged Particle Models (1974), March 1975
SP-8123	The Environment of Titan (1975), July 1976

STRUCTURES

SP-9011	Buffeting During Atmospheric Ascent, revised November 1970
SP-8002	Flight-Loads Measurements During Launch and Exit, revised June 1972
SP-8003	Flutter, Buzz, and Divergence, July 1964
SP-8004	Panel Flutter, revised June 1972
SP-8006	Local Steady Aerodynamic Loads During Launch and Exit, May 1965
SP-8007	Buckling of Thin-Walled Circular Cylinders, revised August 1968
SP-8008	Prelaunch Ground Wind Loads, November 1965
SP-8009	Propellant Slosh Loads, August 1968
SP-8012	Natural Vibration Modal Analysis, September 1968
SP-8014	Entry Thermal Protection, August 1968
SP-8019	Buckling of Thin-Walled Truncated Cones, September 1968
SP-8022	Staging Loads, February 1969
SP-8029	Aerodynamic and Rocket-Exhaust Heating During Launch and Ascent, May 1969
SP-8031	Slosh Suppression, May 1969

SP-8032	Buckling of Thin-Walled Doubly Curved Shells, August 1969
SP-8035	Wind Loads During Ascent, June 1970
SP-8040	Fracture Control of Metallic Pressure Vessels, May 1970
SP-8042	Meteoroid Damage Assessment, May 1970
SP-8043	Design–Development testing, May 1970
SP-8044	Qualification testing, May 1970
SP-8045	Acceptance testing, April 1970
SP-8046	Landing Impact Attenuation for Non-Surface-Planning Landers, April 1970
SP-8050	Structural Vibration Prediction, June 1970
SP-8053	Nuclear and Space Radiation Effects on Materials, June 1970
SP-8054	Space Radiation Protection, June 1970
SP-8055	Prevention of Coupled Structure-Propulsion Instability (Pogo), October 1970
SP-8056	Flight Separation Mechanisms, October 1970
SP-8057	Structural Design Criteria Applicable to a Space Shuttle, revised March 1972
SP-8060	Compartment Venting, November 1970
SP-8061	Interaction with Umbilicals and Launch Stand, August 1970
SP-8062	Entry Gasdynamic Heating, January 1971
SP-8063	Lubrication, Friction, and Wear, June 1971
SP-8066	Deployable Aerodynamic Deceleration Systems, June 1971
SP-8068	Buckling Strength of Structural Plates, June 1971
SP-8072	Acoustic Loads Generated by the Propulsion System, June 1971
SP-8077	Transportation and Handling Loads, September 1971
SP-8079	Structural Interaction with Control Systems, November 1971

SP-8082	Stress-Corrosion Cracking in Metals, August 1971
SP-8083	Discontinuity in Metallic Pressure Vessels, November 1971
SP-8095	Preliminary Criteria for the Fracture Control of Space Shuttle Structures, June 1971
SP-8099	Combining Ascent Loads, May 1972

GUIDANCE AND CONTROL

SP-8015	Guidance and Navigation for Entry Vehicles, November 1968
SP-8016	Effects of Structural Flexibility on Spacecraft Control Systems, April 1969
SP-8018	Spacecraft Magnetic Torques, March 1969
SP-8024	Spacecraft Gravitational Torques, May 1969
SP-8026	Spacecraft Star Trackers, July 1970
SP-8027	Spacecraft Radiation Torques, October 1969
SP-8028	Entry Vehicle Control, November 1969
SP-8033	Spacecraft Earth Horizon Sensors, December 1969
SP-8034	Spacecraft Mass Expulsion Torques, December 1969
SP-8036	Effects of Structural Flexibility on Launch Vehicle Control Systems, February 1970
SP-8047	Spacecraft Sun Sensors, June 1970
SP-8058	Spacecraft Aerodynamic Torques, January 1971
SP-8059	Spacecraft Attitude Control During Thrusting Maneuvers, February 1971
SP-8065	Tubular Spacecraft Booms (Extendible, Reel Stored), February 1971
SP-8070	Spaceborne Digital Computer Systems, March 1971
SP-8071	Passive Gravity-Gradient Libration Dampers, February 1971

SP-8074	Spacecraft Solar Cell Arrays, May 1971
SP-8078	Spaceborne Electronic Imaging Systems, June 1971
SP-8086	Space Vehicle Displays Design Criteria, March 1972
SP-8098	Effects of Structural Flexibility on Entry Vehicle Control Systems, June 1972
SP-8102	Space Vehicle Accelerometer Applications, December 1972

CHEMICAL PROPULSION

SP-8025	Solid Rocket Motor Metal Cases, April 1970
SP-8039	Solid Rocket Motor Performance Analysis and Prediction, May 1971
SP-8041	Captive-Fired Testing of Solid Rocket Motors, March 1971
SP-8048	Liquid Rocket Engine Turbopump Bearings, March 1971
SP-8051	Solid Rocket Motor Igniters, March 1971
SP-8052	Liquid Rocket Engine Turbopump Inducers, May 1971
SP-8064	Solid Propellant Selection and Characterization, June 1971
SP-8073	Solid Propellant Grain Structural Integrity Analysis, June 1973
SP-8075	Solid Propellant Processing Factors in Rocket Motor Design, October 1971
SP-8076	Solid Propellant Grain Design and Internal Ballistics, March 1972
SP-8080	Liquid Rocket Pressure Regulators, Relief Valves, Check Valves, Burst Disks, and Explosive Valves, March 1973
SP-8081	Liquid Propellant Gas Generators, March 1972
SP-8087	Liquid Rocket Engine Fluid-Cooled Combustion Chambers, April 1972
SP-8088	Liquid Rocket Metal Tanks and Tank Components, May 1974
SP-8090	Liquid Rocket Actuators and Operators, May 1973

SP-8094	Liquid Rocket Valve Components, August 1973
SP-8097	Liquid Rocket Valve Assemblies, November 1973
SP-8100	Liquid Rocket Engine Turbopump Gears, March 1974
SP-8101	Liquid Rocket Engine Turbopump Shafts and Couplings, September 1972
SP-8107	Turbopump Systems for Liquid Rocket Engines, August 1974
SP-8109	Liquid Rocket Engine Centrifugal Flow Turbopumps, December 1973
SP-8110	Liquid Rocket Engine Turbines, January 1974
SP-8113	Liquid Rocket Engine Combustion Stablization Devices, November 1974
SP-8114	Solid Rocket Thrust Vector Control, December 1974
SP-8115	Solid Rocket Motor Nozzles, June 1975

NASA-Langley, 1976